Hindawi
International Journal of Antennas and Propagation
Volume 2022, Article ID 8769164, 7 pages
https://doi.org/10.1155/2022/8769164

Research Article

Miniaturized Wide Scanning Angle Phased Array Using EBG Structure for 5G Applications

Xiumei Shen,[1] **Kun Xue**,[1] **Xinggang Tang**,[1] **and Yuqi He**[2]

[1] *School of Mechatronic Engineering, Xi'an Technological University, Xi'an, China*
[2] *National Key Laboratory on Antennas and Microwave Technology, School of Electronic Engineering, Xidian University, Xi'an, China*

Correspondence should be addressed to Xiumei Shen; shenxiumei@xatu.edu.cn

Received 20 October 2022; Revised 17 November 2022; Accepted 18 November 2022; Published 2 December 2022

Academic Editor: Mohammad Alibakhshikenari

This article presents a miniaturized wide-angle scanning phased array for fifth-generation (5G) application. A subarray of two closely packed patch antennas on electromagnetic bandgap structure (EBG) ground with the operating bandwidth of 26–29 GHz is used as the basic module of the linear array, which contains four equally spaced subarrays. The existence of the EBG ground enables the array to be compact in size ($3.2 \times 0.6 \times 0.12\lambda_L{}^3$), yet the mutual coupling between each element can reach to more than 22 dB within the whole band of interest. The EBG structures also contribute to the wide element radiation pattern of the aperiodic array and consequently the wide scanning angle performance of the array. The range of the main beam scan with EBG structure can reach from −70° to 70° with more than 6 dB side lobe levels (SLLs) at 26.5 GHz with 3 dBi scanning gain loss. This proposed method enabling the array to be compact and wide in scanning angle is very attractive for 5G mobile terminal applications.

1. Introduction

After several decades of evolution, the wireless communication system has developed from the first generation (1G) to the current fourth generation (4G). With the everlasting demand for higher data rate, the application of the fifth-generation (5G) communication system is urgent to be applied with both sub-6 GHz and millimeter-wave bands [1, 2]. Millimeter-wave technology is considered to be the most critical technique to achieve a high data rate because it has a much broader absolute bandwidth. However, millimeter-wave bands have more challenges in aspects of space, propagation loss, efficiency, and coverage compared with sub-6 GHz bands. Therefore, the antenna array will be the development trend at both the base stations and application of terminals, for its high gain and beam steering capabilities [3, 4]. In portable terminal products, there is very limited space reserved for millimeter phased arrays because of the existence of other antennas, as well as the complex electromagnetic environment. Therefore, the antenna arrays at millimeter-wave band with high gain, wide scanning angle, and compact size are highly demanded.

There are two ways to generate beams with wide scanning angle, small array spacing, and wide radiation. However, the small space between elements in the antenna array will cause strong mutual coupling, which will deteriorate performance of the antenna and cause scanning blindness [5]. It is essential to reduce the coupling between antennas while reducing the spacing. Before this work, there are many mutual coupling reduction methods to be proposed, for example, decoupling networks [6, 7], periodic structures such as electromagnetic bandgap structures [8, 9], parasitic decoupling structures [10], and dummy elements [11].

Many reports such as [10, 12–21] focus on reducing the profile and broadening scanning angle of antenna arrays in millimeter-wave bands. In [13], to obtain a wider coverage at 28 GHz, two subarrays of cavity-backed slot antennas placed parallelly on both sides of the phone are employed with the scan angle of ±60°. The same working mechanism is adopted in [14, 15] too, for which the switchable 3D-coverage phased arrays for 28 GHz mobile terminal applications are designed. The antenna array occupies the whole upper part of the phone box. And the impedance bandwidth of the phased

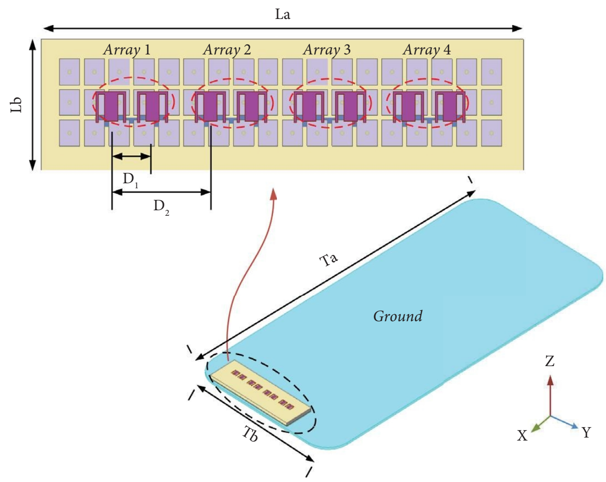

Figure 1: Structure of eight-element phased array antenna ($L_a = 37$ mm, $L_b = 7$ mm, $D1 = 3.4$ mm, $D2 = 7.6$ mm, $T_a = 150$ mm, and $T_b = 70$ mm).

array antenna [14] is quite limited (1 or 2 GHz). There are many endfire antennas preferred in the mobile handsets that have been reported in [17–19]. In [18], a compact dual-polarized endfire antenna array constructed by a compact open-ended cavity with cavity mode for vertical and horizontal polarization (VP and HP) radiation has the beam scanning coverage of ±50° with realized gain above 7 dBi at 27 GHz. Most of them suffer from complex feeding system, making them take up too much space or limited scanning angle for 5G communications.

To solve the problem mentioned above, a subarray of two closely packed patch antennas on electromagnetic bandgap structure (EBG) ground with an operating bandwidth of 26–29 GHz [9] is used as the basic module to form the linear array in this paper. The periodic structure in [9] not only reduces the mutual coupling and makes the volume compact but also delivers grating lobe suppression and higher gain enhancement [22] compared to the array without EBG. All of these effects can improve the scanning angle.

The remaining parts of the paper will be arranged as follows: Part II focuses on the design and analysis of the antenna array, which presents the configuration of the proposed array and the basic simulated and measured performances. The detail characteristics of wide-angle scanning will be displayed in part III. Part IV concludes the whole paper.

2. Optimized Parameters of Wide-Angle Scanning Phased Array

Figure 1 displays the structure of the proposed wide-angle scanning phased array for fifth-generation (5G) application. As illustrated, the whole eight-element array is configured in an asymmetric manner, in which four subarrays with two elements are linearly arranged. The array is fabricated on Rogers 4003 substrate ($\varepsilon r = 3.557$). Figures 2(a) and 2(b) show the configuration of the subarray of two closely packed patch antennas on electromagnetic bandgap structure (EBG) ground with an operating bandwidth of 26–29 GHz, which is already introduced in [9]. However, in [9], only the mutual coupling reduction property of the EBG ground is discovered. As mentioned in [23], the wide-beam of the element can expand the scanning coverage of the phased array. In order to demonstrate that the proposed EBG structure can effectively broaden its radiation pattern, the field distributions and radiation patterns in the H-plane are proposed in Figures 2(c) and 2(d). The coverage of electric field of the antenna on EBG ground is larger compared with antenna on normal ground. And the antenna on the EBG ground has a maximum gain of 6.9 dBi located at 45° and a half-power beam coverage of 115°. In contrast, the antenna on the common ground shows radiation with the main beam towards 20° and half-power beam coverage of 70°. Moreover, the Ant 1 on the left has its main beam tilt to the right side and the Ant 2 on the right radiate to the left.

It is known from [23, 24] that aperiodic array shows the advantage of high spatial resolution and wide-angle scanning without grating lobes compared with equally spaced arrays. Then, an aperiodic linear array with 4 subarrays of two closely packed patch antennas on electromagnetic bandgap structure (EBG) ground is designed. The spacing between the subarrays is optimized ($D2 = 7.6$ mm) to ensure the proper matching and isolation performances of all antenna feeding ports. The simulated and measured reflection coefficients of elements in the array are given in Figures 3(b) and 3(c), respectively. Figure 3(b) presents the simulated −10 dB impedance bandwidth of the antennas covering from 26 GHz to 29 GHz. All of the simulation isolations are less than −20 dB during the working band. The measured resonant frequency of the ant1 to ant4 (at 27 GHz) in Figure 3(c) slightly deviates from the simulated result. Also, the measured S12, S23, and S34 in Figure 3(d) confirm a good isolation characteristic, which is less than 20 dB, in the operating band. The performance of the Ant5–Ant8 is similar to Ant1–Ant4 due to the distribution symmetry. All the results exhibit good impedance matching level and low mutual coupling between subarrays at operational frequency. There are small frequency shift and abnormal points at 28.5 GHz in the measurement results, which may be due to slight fabrication and cable inaccuracy.

Besides, Figure 3(a) shows the prototype of the fabricated antenna array. The radiation pattern of the subarrays (array 1-array 4) in the phased scanning array is shown in Figure 4(a). The proposed antenna subarrays have a wide scan angle of 115° in the H-plane with gain loss 3 dBi. The results indicate that the wide-beam pattern characteristics are relatively stable in the array.

3. Scanning Performance of the Phased Antenna Array

In general, the array factor of the uniform linear array is as follows:

$$\mathrm{fa}(\theta) = \sum N - 1\, n = 0\mathrm{Inej}\,(\mathrm{kzncos}\theta). \quad (1)$$

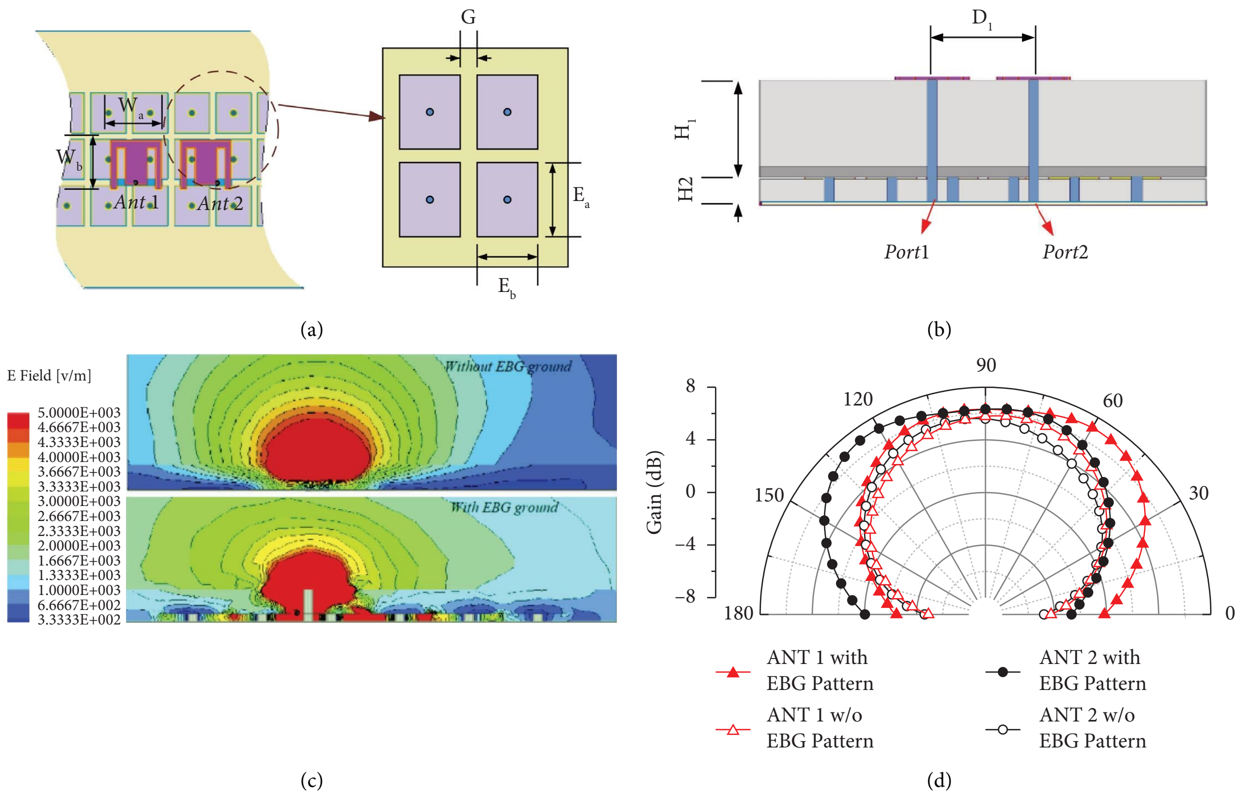

Figure 2: Configuration of the subarray with the EBG ground (a) top view; (b) side view [9] ($W_a = 2.5$ mm, $W_b = 2.4$ mm, $G = 0.35$ mm, $E_a = 2.1$ mm, and $E_b = 1.7$ m). (c) Simulated E-field distributions of the antenna (port1 excited) without and with the EBG ground. (d) Simulated radiation pattern (H-plane) of subarray when Ant 1 and Ant 2 is independently excited, respectively.

For a linear array with unequal spacing [25], $Z0 = 0$, $Z1 = d1$, $Z2 = d2$, $d1 \neq 2d2$, that is, $Z2n = nd2$, $Z2n + 1 = nd2 + d1$ in this paper. We have

$$\text{fa}(\theta) = \frac{\sum \text{N} - 1}{2} n = 0 e j (\text{knd2} \cos \theta) (I2n + I2n + 1 e j (\text{knd1} \cos \theta)). \tag{2}$$

According to formula (2), the array factor of the unequal spacing array is the superposition of two isometric arrays. For phase sweep performance in this paper, the uniform input amplitudes and different phases are applied. The phase differences $\Delta\phi = \Phi_{2n} - \Phi_{2n-1}$ in subarrays and $\Delta\phi = \Phi_{2n+1} - \Phi_{2n-1}$ during subarrays are deduced [24] and calculated phased inputs from Ant 1 to Ant 8 are optimized in Table 1.

The 2D main beam steering characteristic of the phased array (without phone ground) in different scanning angles from 0° to 70° at 26 GHz is depicted in Figure 4(b) with a maximum gain of 14.4 dBi. As illustrated, the gain levels are smoothly (14 dBi) in the range from 0° to 35° with less than 1 dB gain variation. In comparison, the gain levels between 35° and 70° have dropped to 12 dBi approximately. And the sidelobe levels are approximately −13 dB at angle of 0° and −6 dB at angle of 70°. It is obvious that the scan of positive and negative angles is symmetric. The 8-element phased array has demonstrated good beam steering characteristics during the range of ±70°.

In order to demonstrate the influence of the EBG structure, Figure 4(c) shows the 2D main beam steering characteristic of the phased array without EBG ground in different scanning angles at 26 GHz at free space. The phased array without EBG ground has the beam steering characteristic from 0° to 55° with 3 dBi gain variation. When the scanning beam reaches over 55°, the side lobe value of the scanning pattern increases more than 10 dBi. The comparison of gain performance at different steering angle of the array with and without EBG structures is given in Figure 4(d). It can be seen that the gain of the proposed phased array is higher than the array without EBG ground when the scan angle is larger than 50°.

Finally, to demonstrate the advantageous performance of the proposed array, a comparison with recently research papers is tabulated in Table 2. Several antenna performances, such as antenna sizes, number of arrays, the peak-gain, scanning range, distance between elements, and working band, are listed. The proposed antenna array features a lower profile, a wider wide-angle scan, and a better mutual coupling reduction in the operation frequency band.

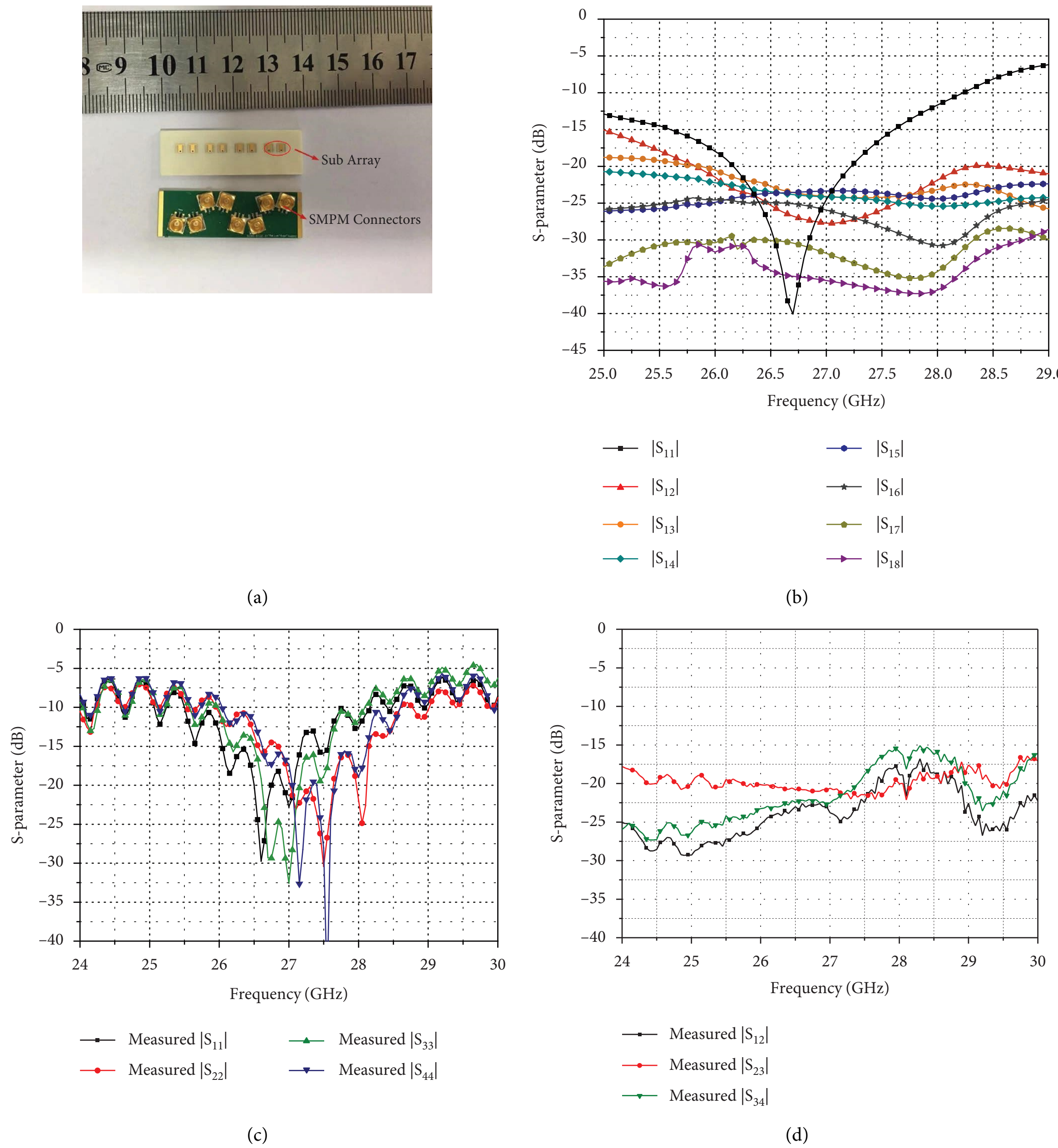

Figure 3: (a) The prototype of the fabricated antenna array; (b) simulated S-parameters of the proposed antenna array; (c) measured return loss of the proposed antenna; (d) measured isolation of the proposed antenna.

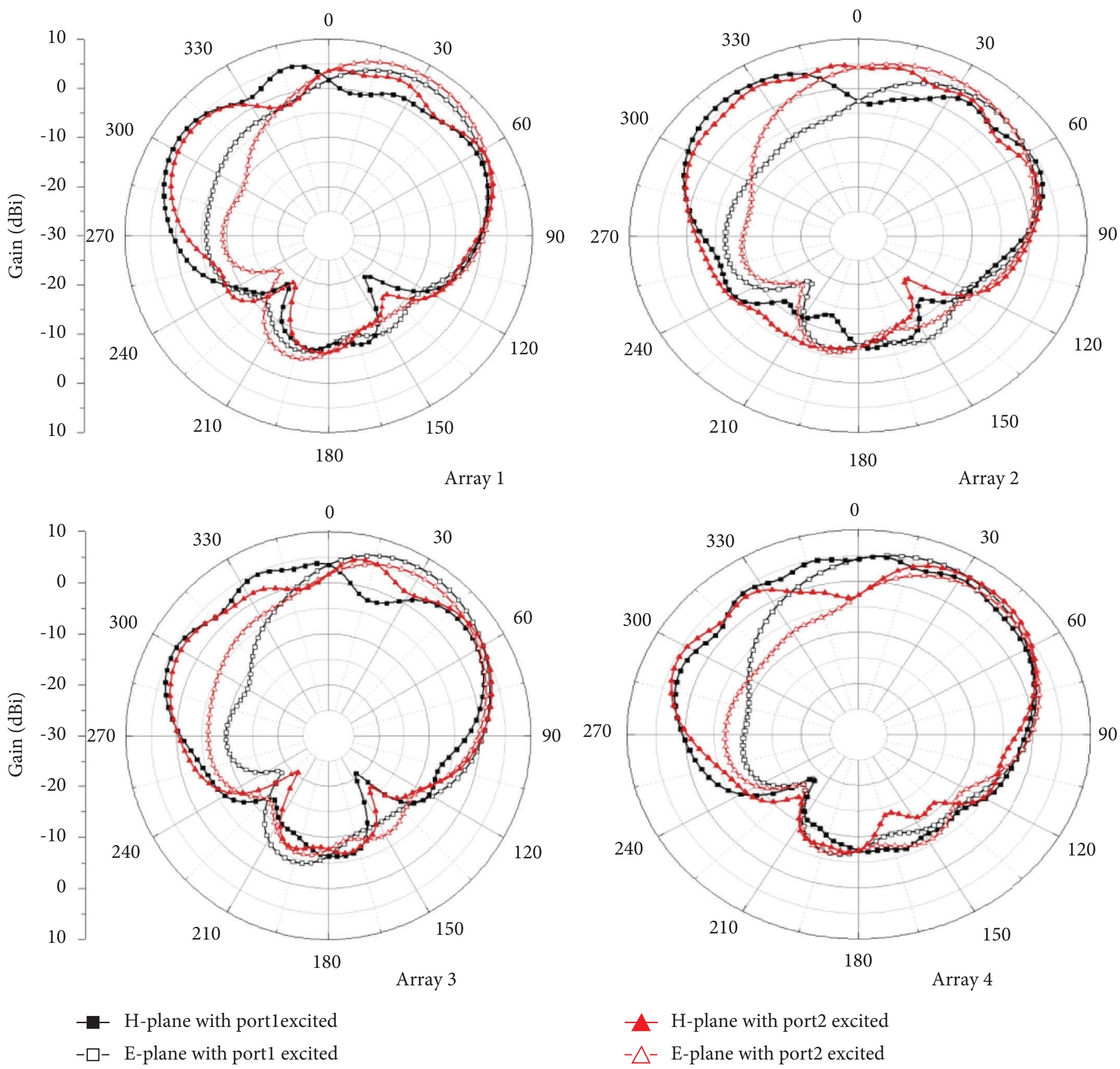

(a)

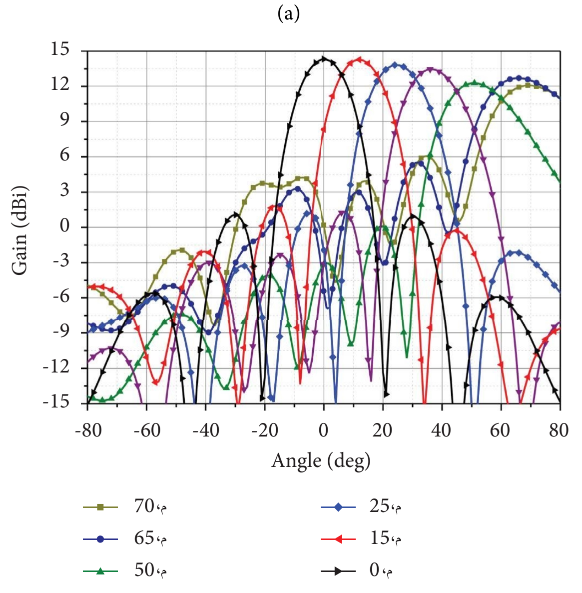

(b)

Figure 4: Continued.

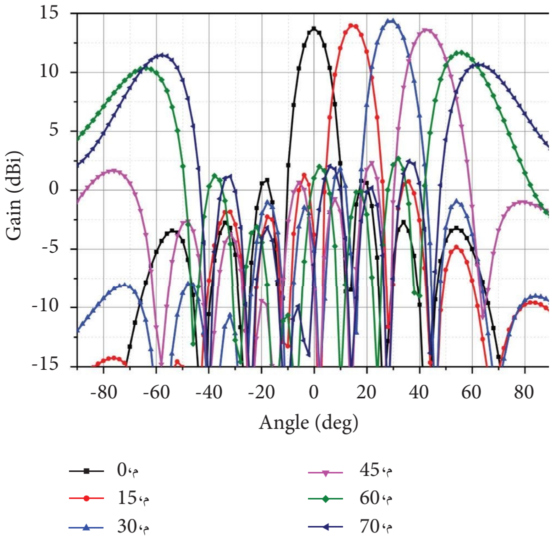

(c)

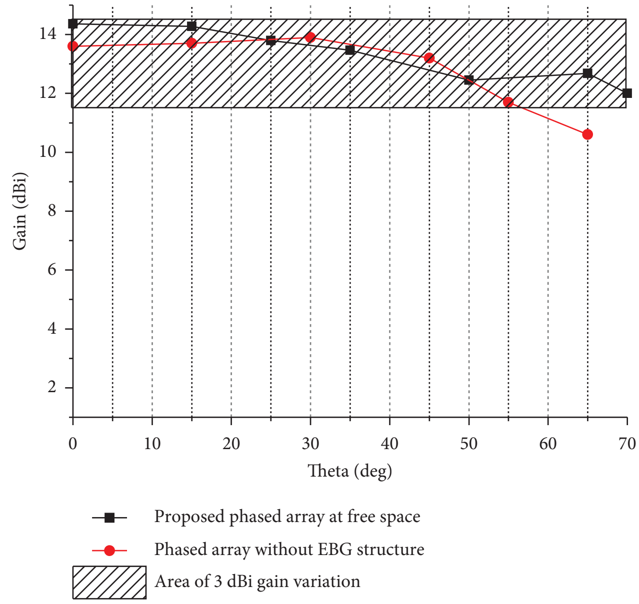

(d)

Figure 4: (a) The radiation patterns of the Array1, Array2, Array3, and Array4 in the E and H-plane. (b) The simulation 2D radiation patterns of the 8-element phased array with EBG ground in different scanning angles. (c) The simulation 2D radiation patterns of the 8-element phased array without EBG ground in different scanning angles. (d) The simulation gain comparison at different scanning angles of the array with and without EBG structures.

Table 1: Calculated phase inputs of the full arrays (unit: degree).

Angle	Φ_1	Φ_2	Φ_3	Φ_4	Φ_5	Φ_6	Φ_7	Φ_8
0	0	0	0	0	0	0	0	0
15	0	−25	−55	−80	−110	−135	−165	−14
25	0	−50	−108	−158	143	94	35	−27
35	0	−72	−158	130	43	−29	−115	173
50	0	−92	156	64	−47	−140	110	16
65	0	−118	100	−17	−160	−83	−60	−176
70	0	−140	85	−55	170	32	−104	115

Table 2: Comparison of proposed antenna performance with recent antenna designs.

	Frequency (GHz)	Ant. num.	Ant. size (λ_L^3)	Coverage	C to C (λ_L)
[10]	27–29	8	$3.7 \times 0.9 \times 0.16\lambda_L^3$	70° (GV ≤ 5 dBi)	$0.5\lambda_L$
[15]	21–22	8	$3.8 \times 0.35 \times 0.13\lambda_L^3$	60° (GV ≤ 3 dBi)	$0.46\lambda_L$
[20]	24–29.5	8	$5.1 \times 0.64 \times 0.02\lambda_L^3$	N/A	$0.64\lambda_L$
[21]	22–32	4	$1.7 \times 1.5 \times 0.45\lambda_L^3$	35° (GV ≤ 3 dBi)	$0.424\lambda_L$
[14]	27.5–30	8	$4.6 \times 0.36 \times 0.14\lambda_L^3$	60° (GV ≤ 3 dBi)	$0.6\lambda_L$
[17]	26–32	8	$3.8 \times 0.52 \times 0.14\lambda_L^3$	60° (GV ≤ 3 dBi)	$0.5\lambda_L$
Proposed	26–29	8	$3.2 \times 0.6 \times 0.12\lambda_L^3$	70° (GV ≤ 3 dBi)	$0.29\lambda_L$ and $0.36\lambda_L$

Notes. GV: gain variation. C to C spacing: element center to center spacing; λ_L is the free-space wavelength at the lowest frequency of the operating bands.

4. Conclusion

In this paper, a miniaturized wide-angle beam steering array is designed and investigated. The proposed antenna array is compact in size, yet the mutual coupling between each element can reach to more than 22 dB within the whole band of interest. From the scanning angle results, the proposed phased array has a superior performance of beam scanning from -70° to $+70^{\circ}$ with less than 3 dBi gain variation. The proposed low profile wide-angle beam steering array is one of the potential design methods that can be adopted for 5G applications.

Data Availability

Data are available on request.

Conflicts of Interest

The authors declare that they have no conflicts of interest.

References

[1] T. Osseiran, "Mobile and wireless communications system for 2020 and beyond (5G)," *Research views on IMT beyond*, vol. 12, 2020.

[2] T. S. Rappaport, S. Sun, R. Mayzus et al., "Millimeter wave mobile communications for 5G cellular: it will work," *IEEE Access*, vol. 1, pp. 335–349, 2013.

[3] C. Narayan, *Antennas and Propagation*, Technical Publications, 2007.

[4] T. S. Rappaport, F. Gutierrez, E. Ben-Dor, J. N. Murdock, Y. Qiao, and J. I. Tamir, "Broadband millimeter-wave propagation measurements and models using adaptive-beam antennas for outdoor urban cellular communications," *IEEE Transactions on Antennas and Propagation*, vol. 61, no. 4, pp. 1850–1859, 2013.

[5] L. Savy and M. Lesturgie, "Coupling Effects in MIMO Phased Array," in *Proceedings of the IEEE Radar Conf. (RadarConf)*, pp. 1–6, Philadelphia, PA, USA, May 2016.

[6] Y.-M. Zhang, Q.-C. Ye, G. F. Pedersen, and S. Zhang, "A simple decoupling network with filtering response for patch antenna arrays," *IEEE Transactions on Antennas and Propagation*, vol. 69, no. 11, pp. 7427–7439, Nov, 2021.

[7] M. Li, M. Wang, L. Jiang, and L. K. Yeung, "Decoupling of antennas with adjacent frequency bands using cascaded decoupling network," *IEEE Transactions on Antennas and Propagation*, vol. 69, no. 2, pp. 1173–1178, Feb, 2021.

[8] M. J. Al-Hasan, T. A. Denidni, and A. R. Sebak, "Millimeter-wave compact EBG structure for mutual coupling reduction applications," *IEEE Transactions on Antennas and Propagation*, vol. 63, no. 2, pp. 823–828, 2015.

[9] X. Shen, Y. Liu, L. Zhao, G. L. Huang, X. Shi, and Q. Huang, "A miniaturized microstrip antenna array at 5G millimeter-wave band," *IEEE Antennas and Wireless Propagation Letters*, vol. 18, no. 8, pp. 1671–1675, 2019.

[10] S. Zhang, X. Chen, I. Syrytsin, and G. F. Pedersen, "A planar switchable 3-D-coverage phased array antenna and its user effects for 28-GHz mobile terminal applications," *IEEE Transactions on Antennas and Propagation*, vol. 65, no. 12, pp. 6413–6421, Dec, 2017.

[11] L. Zhao and K. L. Wu, "A decoupling technique for four-element symmetric arrays with reactively loaded dummy elements," *IEEE Transactions on Antennas and Propagation*, vol. 62, no. 8, pp. 4416–4421, Aug, 2014.

[12] C.-M. Liu, X. Shaoqiu, and X.-L. Zhang, "A compact, low-profile wire antenna applied to wide-angle scanning phased array," *IEEE Antennas and Wireless Propagation Letters*, vol. 17, no. 3, pp. 1–392, 2018.

[13] I. Syrytsin, S. Zhang, G. F. Pedersen, and A. S. Morris, "Compact quad-mode planar phased array with wideband for 5G mobile terminals," *IEEE Transactions on Antennas and Propagation*, vol. 66, no. 9, pp. 4648–4657, 2018.

[14] B. Yu, K. Yang, C. Y. D. Sim, and G. Yang, "A novel 28 GHz beam steering array for 5G mobile device with metallic casing application," *IEEE Transactions on Antennas and Propagation*, vol. 66, no. 1, pp. 462–466, 2018.

[15] N. Ojaroudiparchin, M. Shen, S. Zhang, and G. F. Pedersen, "A switchable 3-D-coverage-phased array antenna package for 5G mobile terminals," *IEEE Antennas and Wireless Propagation Letters*, vol. 15, pp. 1747–1750, 2016.

[16] M. Masoumi, H. R. Dalili Oskouei, M. Mohammadi Shirkolaei, and A. R. Mirtaheri, "Substrate integrated waveguide leaky wave antenna with circular polarization and improvement of the scan angle," *Microwave and Optical Technology Letters*, vol. 64, no. 1, pp. 137–141, 2022.

[17] M. Stanley, Y. Huang, T. Loh, Q. Xu, H. Wang, and H. Zhou, "A high gain steerable millimeter-wave antenna array for 5G smartphone applications," in *Proceedings of the 2017 11th European Conference on Antennas and Propagation (EUCAP)*, pp. 1311–1314, ParisChina, April 2017.

[18] L. Sun, Y. Li, and Z. Zhang, "Wideband dual-polarized endfire antenna based on compact open-ended cavity for 5G mm-wave mobile phones," *IEEE Transactions on Antennas and Propagation*, vol. 70, no. 3, pp. 1632–1642, March 2022.

[19] X. Cheng, Y. Yao, T. Tomura et al., "A compact multi-beam end-fire circularly polarized septum antenna array for millimeter-wave applications," *IEEE Access*, vol. 6, pp. 62784–62792, 2018.

[20] C. X. Mao, M. Khalily, P. Xiao, T. W. C. Brown, and S. Gao, "Planar sub-millimeter-wave array antenna with enhanced gain and reduced sidelobes for 5G broadcast applications," *IEEE Transactions on Antennas and Propagation*, vol. 67, no. 1, pp. 160–168, 2019.

[21] B. Yang, Z. Yu, Y. Dong, J. Zhou, and W. Hong, "Compact tapered slot antenna array for 5G millimeter-wave massive MIMO systems," *IEEE Transactions on Antennas and Propagation*, vol. 65, no. 12, pp. 6721–6727, Dec, 2017.

[22] M. Mohammadi Shirkolaei, H. R. Dalili Oskouei, and M. Abbasi, "Design of 1∗4 microstrip antenna array on the human thigh with gain enhancement," *IETE Journal of Research*, vol. 20, pp. 1–7, 2021.

[23] C. A. Balanis, *Antenna Theory, Analysis and Design*, pp. 96–112, Wiley, New York, USA, 2nd edit edition, 1997.

[24] L. Cen, W. Ser, Z. L. Yu, S. Rahardja, and W. Cen, "Linear sparse array synthesis with minimum number of sensors," *IEEE Transactions on Antennas and Propagation*, vol. 58, no. 3, pp. 720–726, Mar. 2010.

[25] A. Ishimaru, "Unequally spaced arrays based on the Poisson sum formula," *IEEE Transactions on Antennas and Propagation*, vol. 62, no. 4, pp. 1549–1554, 2014.